Structural Characterization Composites Based on Butadiene Rubber and Expanded Perlite

Nada Edres , Irada Buniyat-zadeh , Sinan Mehmet Turp , Mustafa Soylak , Solmaz Aliyeva , Nurlana Binnetova , Naila Guliyeva , Sevinj Mammadyarova , Rasim Alosmanov *

Posted Date: 20 October 2023

doi: 10.20944/preprints202310.1338.v1

Keywords: butadiene; expanded perlite; modification; composite; structural characterization

Article

Structural Characterization Composites Based on Butadiene Rubber and Expanded Perlite

Nada Edres [1,2], Irada Buniyat-zadeh [2], Sinan Mehmet Turp [3], Mustafa Soylak [4,5,6], Solmaz Aliyeva [7], Nurlana Binnetova [8], Naila Guliyeva [9], Sevinj Mammadayarova [10] and Rasim Alosmanov [2,*]

[1] Department of Chemistry, Faculty of Education, Khartum University; nadaedres2010@gmail.com
[2] Department of High-molecular Compounds Chemistry, Faculty of Chemistry, Baku State University; i_buniatzade@mail.ru
[3] Department Chemical & Chemical Processing Technology, Tatvan Vocat High School, Bitlis Eren University; smturp@gmail.com
[4] Erciyes University, Faculty of Sciences, 38039, Kayseri, Turkey; soylak@erciyes.edu.tr
[5] Erciyes University, Technology Research and Application Center (ERU-TAUM), 38039, Kayseri, Turkey; soylak@erciyes.edu.tr
[6] Turkish Academy of Sciences (TUBA), 06670, Ankara, Turkey; soylak@erciyes.edu.tr
[7] Women Researchers Council, Azerbaijan State University of Economics (UNEC), Istiglaliyyat 6, AZ1001 Baku, Azerbaijan; solmaz.aliyeva@yahoo.com
[8] Department of Ecology, Faculty of water management and Engineering Communication Systems, Azerbaijan University of Architecture and Construction; binnatova_nurlana@rambler.ru
[9] School of High Technologies and Innovative Engineering, Western Caspian University; nailya.kulieva.76@mail.ru
[10] Nano Research Laboratory, Baku State University, 1148, Baku, Azerbaijan; sevinc.memmedyarova@inbox.ru
* Correspondence: r_alosmanov@rambler.ru

Abstract: The article presents a method for obtaining new composites using a well-known mineral, expanded perlite (EP), and an industrial polymer, butadiene rubber (BR). For the design of composites, a joint oxidative chlorophosphorylation reaction of BR and EP (as well as BR and modified EP) was carried out, and the modifications obtained from this reaction were further hydrolyzed. The structure and morphology of the obtained samples were characterized in detail using Fourier transform infrared spectroscopy, ultraviolet-visible spectroscopy, X-ray powder diffraction, as well as scanning electron microscopy, and energy-dispersive X-ray analysis. EP and BR were separately modified with a similar reaction and characterized for data interpretation.

Keywords: butadiene; expanded perlite; modification; composite; structural characterization

1. Introduction

Expanded perlite (EP) mainly consists of about 70-75 % silicon dioxide, aluminum oxide, and oxides of other metals. It is obtained through calcination at 850-900 °C volcanic glassy hydrated rock perlite, which is a mineral of natural origin. The EP particles have a spherical glass wall with pores of various sizes, are chemically inert, and have low thermal conductivity [1–3]. In the industry, EP is applied in many fields such as horticultural fill, light construction components, environmental and temperature insulators, and in the preparation of flame retardant, acoustic, and filter materials [1,2]. In addition, EP attracts the attention of researchers due to its physical and chemical properties. In several works, scientists have studied the influence of EP waste on the properties of autoclaved aerated concrete [4] and presented a method for using expanded perlite waste as a valuable, high-performance pozzolanic additional binder material [5]. Based on it, a new type of insulating material [6] and magnetic nanocomposite [7] was developed.

Recently, EP/polymer composites have attracted impressive attention due to their attractive mechanical, thermal, and other properties. Like all mineral/polymer composites, the morphological

 doi:10.20944/preprints202310.1338.v1

structure, properties, and effective characteristics of EP/polymer composites depend on the interfacial interaction of EP particles with the polymer matrix, which is affected by the quality of the EP particle dispersion and the chemical compatibility between the EP particles and the polymer matrix [8]. As expected, all this is determined by the methods of composite synthesis.

Polypropylene/amorphous aluminosilicate rock composites containing 0-20 wt% raw perlite and EP were synthesized by extrusion-compression molding by Esabbir et al. [9]. The method provides good dispersion, distribution, and interfacial adhesion of EP in the polymer matrix. In general, the mechanical properties and thermal stability of the polymer were improved with the addition of EP. It is known that epoxy resin and EP-based composites with desirable ablative properties can be prepared by exploiting the mechanical mixing method and then gravity casting. From this study, it was observed that EP improved the ablative properties of epoxy resin [10]. A compression molding technique was applied by Arifuzzaman et al. to produce a new composite material using EP and recycled Styrofoam. The prepared material has low weight, sound, and heat-insulating properties [11]. A method for the production of EP-filled high-density polyethylene (HDPE) composites by adding different weight fractions (5, 10, 20, and 30 wt%) of EP powder to the HDPE matrix using a thermokinetic mixer is known. From the mechanical tests, it was observed that the amount of EP has a different effect on the individual properties of the composites [12]. Polyamide 6/acrylonitrile butadiene rubber/EP nanocomposites with various percentages of NBR phase and mineral nanoparticles were prepared using a melt blending process. The peculiarity of this study was that two types of polymers (thermoplastic and elastomer) were used for the preparation of composites. The results confirmed that changing the percentage ratio of elastomer and EP nanoparticles makes it possible to obtain composites with optimal mechanical properties [13]. Akkaya et al. synthesized a novel poly(acrylamide-EP) composite through free radical polymerization. It was revealed that acrylamide plays the role of a crosslinking agent for perlite and the composite has an increased chemical resistance [14]. In another study, the adsorption properties of the composite against Tb^{3+} ions from aqueous solutions were investigated [15].

Thus, it is clear from the reviewed studies that researchers have proposed both physical [9–13] and chemical synthesis methods [14,15] for the design of EP/Polymer composites.

In the present study, industrial polymer-butadiene rubber (BR) was chosen as the polymer component for the preparation of the EP/polymer composite. The synthesis procedure consisted of carrying out a joint reaction of oxidative chlorophosphorylation (OxCh) of BR and EP followed by hydrolysis of the resulting intermediate composite. It should be noted that the OxCh reaction previously was used to synthesize phosphorus- and phosphorus/nitrogen-containing functional polymers (based on BR), as well as BR hybrid composites with graphene nanoplates and bentonite [16–18]. The scientific novelty of the work lies in the fact that the OxCh reaction was used for the first time for the synthesis of an EP/polymer composite. The structures of new composites were studied using FTIR, XRD, UV-Vis, and SEM-EDX methods. The results of the study of phosphorus-containing BR (without filler) synthesized by the same method are also presented for comparison. In addition, the preparation of composites of this type is because silanol groups are very sensitive to the presence of other organic molecules that can interact with them. These are groups that are present on the EP surface and can be attracted to organic molecules (in this case, rubber macromolecules).

2. Materials and Methods

2.1. Materials

BR was purchased from Voronezh Synthetic Rubber Manufactory (Russia). It consists of 96-98 % of cis-1,4 units. The EP was purchased from Bitlis (Turkey). Phosphorus trichloride (PCl_3), carbon tetrachloride (CCl_4), and sulfuric acid were used without further purification (Gorex Analyt GmbH). Oxygen was supplied to the reaction medium by purging through the concentrated sulfuric acid.

2.2. Methods

Preprints (www.preprints.org) | NOT PEER-REVIEWED | Posted: 20 October 2023 doi:10.20944/preprints202310.1338.v1

2.2.1. Synthesis of the first type of composite

The first type of composite was synthesized in two steps.

The first step is the OxCh reaction and was carried out as follows: 5 g of BR was dis-solved in 50 ml of CCl4 in a three-necked round-bottomed flask and 0.5 g of EP was added to this solution. The flask is equipped with a reflux condenser, a thermometer, and a bubbler to supply oxygen gas to the reaction zone. Oxygen is fed into the reaction medium after passing through concentrated sulfuric acid to purify the gas, then PCl_3 is cautiously added to the reaction zone in portions (the weight ratio of BR and PCl_3 is equal to 1:3), and the oxygen supply during the reaction is continuous at a rate of 7 L/h is kept. The nature of the reaction was exothermic, the temperature increased to 50 °C. A dark brown solid was obtained within 3 hours (Figure 1-step 1) and was then separated from the liquid using a distillation under a water pump. As a result, a composite with $-P(O)(Cl)_2$ groups was obtained. This composite contains active P-Cl bonds that are easily hydrolyzed.

In the second step, the hydrolysis process of the $-P(O)(Cl)_2$ composite obtained in the first step was carried out under continuous stirring at 50 °C for 2 hours (Figure 1-step 2). The product obtained at this step is filtered and washed with distilled water and then with acetone until neutral pH. The final product contained $-P(O)(OH)_2$ groups and was dried first in air and then in a vacuum drying oven at 50°C for 2 hours. The resulting composite is abbreviated as EP/PhBR. The synthesis of the composite EP/PhBR is presented in Figure 1.

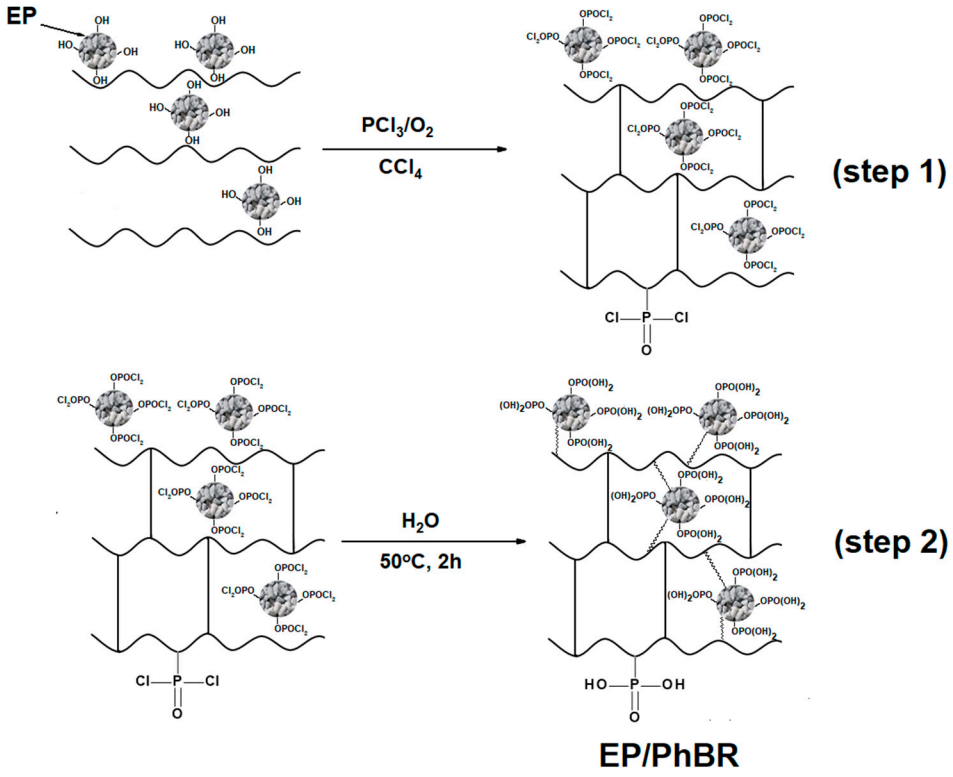

Figure 1. Synthesis scheme of EP/PhBR.

2.2.2. Synthesis of the second type of composite

The second type of composite was synthesized in three steps.

In the first step, EP was added to a three-necked flask with CCl_4 inside, and the flask was equipped with a reflux condenser, a thermometer, and a bubbler to supply oxygen gas to the reaction zone. The amount of EP added (g) is 2% of the CCl_4 volume (ml). The mixture in the flask was kept under continuous stirring and the reaction zone was enriched with oxygen at a rate of 7 l/h. PCl_3 was carefully added to the reaction mixture in a weight ratio of EP to PCl_3 of 1:6. The temperature rose to 38°C, the reaction mixture turned yellowish-white within 40 minutes, and the temperature dropped

Preprints (www.preprints.org) | NOT PEER-REVIEWED | Posted: 20 October 2023 doi:10.20944/preprints202310.1338.v1

to room temperature (Figure 2-step 1). A part of this mixture was taken for analysis, and a 10% solution of pure BR in CCl_4 was added to the remaining part, and PCl_3 was added again in a 1:3 weight ratio (BR : PCl_3) with the same manner (2.2.1. Synthesis of the first type of composite), and the reaction was continued. The temperature of the reaction medium was gradually increased to 48°C and a dark brown solid was obtained in the medium over 4 hours. After this time, the temperature of the reaction medium does not increase with the addition of PCl3, which indicates the completion of the reaction (Figure 2-step 2). After the second step, the solid product in the flask was separated from the liquid phase by a water pump. Then, this sol-id product containing -P(O)$(Cl)_2$ groups were hydrolyzed at 50 °C for 2 hours (Figure 2-step 3), after hydrolysis, the product was washed with deionized water, dried first in the air, and then in a vacuum drying oven. The resulting composite is abbreviated as PhEP/PhBR. The synthesis of the composite PhEP/PhBR is illustrated in Figure 2.

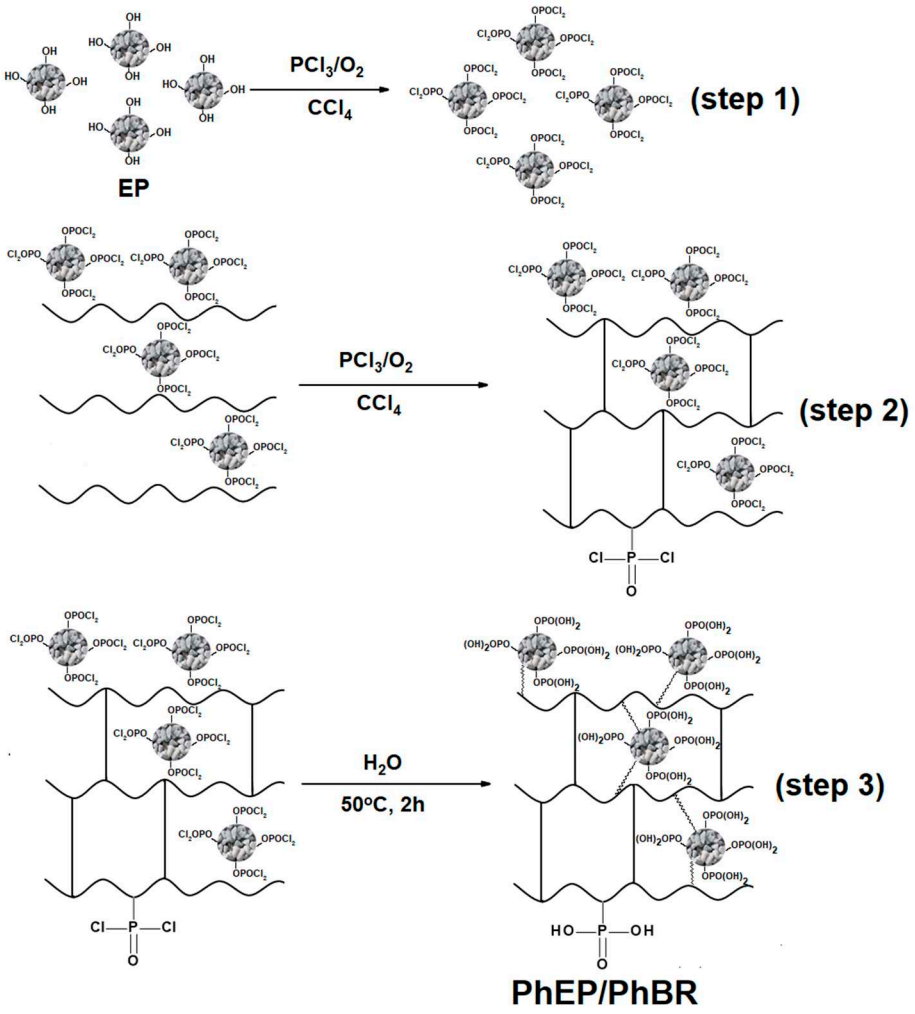

Figure 2. Synthesis scheme of PhEP/PhBR.

2.2.3. Synthesis of PhBR

A viscous solution of 6% BR in CCl_4 was prepared in a three-necked flask equipped with a reflux condenser, a thermometer, and an oxygen gas supplier and kept under stirring. Gaseous oxygen was plugged into the reaction medium at a rate of 7 liters per hour to purge the reaction medium. The reaction started by adding 10 ml of PCl_3 dropwise to the mixture (the first step), the temperature rose to 51 °C, indicating that the reaction was exothermic. After 3 hours a thick brown solid formed in the medium and the temperature dropped to room temperature (Figure 3-step 1)). Thereafter, the liquid phase containing (PCl_3, CCl_4, and $POCl_3$) was separated from the solid by simple distillation connected to a vacuum pump. Next, the solid containing -P(O)$(Cl)_2$ groups were hydrolyzed at 50 °C

Preprints (www.preprints.org) | NOT PEER-REVIEWED | Posted: 20 October 2023 doi:10.20944/preprints202310.1338.v1

for 2 h (Figure 3-step 2), washed with deionized water, and finally dried in air and vacuum **[16]**. The synthesis of the PhBR is shown in Figure 3.

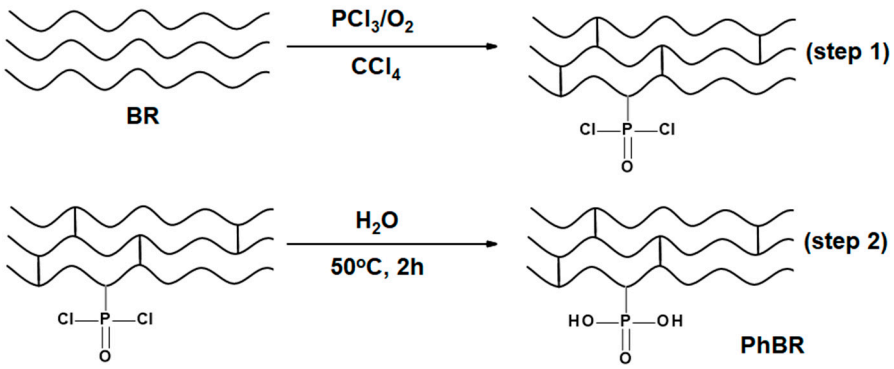

Figure 3. A synthesis scheme of modified BR.

2.2.4. Characterisation techniques

FTIR spectra of all samples were measured using a Perkin Elmer Spectrum 100 FTIR spectrophotometer in the range of 650–4000 cm^{-1}. Its resolution value is 4 cm^{-1} and 4 standard scans were taken. The samples (without using KBr or NaCl) were clamped under the ATR disc and the measurements were taken.

UV-Vis spectroscopy studies of the samples were carried out using the Specord 210 Plus (Analytik Jena, Germany) UV-Vis spectrophotometer in the wavelength range of 190–700 nm. The measurements were carried out using a solid sample holder, which allowed the samples to be studied in the form of powder.

XRD patterns were recorded on a Rigaku Mini Flex 600 X-ray diffractometer (λ=1.54060 Å) using the Ni-filtered Cu Kα radiation with a step width of 0.1° and a scanning speed/duration time of 5°/minute in the 2θ range from 10° to 90°.

The surface morphology of the samples was observed using a field emission scanning electron microscope (Zeiss Gemini 500, Carl Zeiss SMT AG, Germany) after coating with gold (about five nm thick). EDX spectroscopy was used to identify the elements present in the samples.

3. Results and Discussion

It should be noted that the characterization of PhBR has been studied in detail in our previous studies [16,19]. In particular, the existence of a C-O-C bond between macromolecules was proved by the NMR solid phase method [19]. In addition, the presence of C-Cl fragments in the polymer matrix was confirmed by thermogravimetric-mass spectrometric analysis [16]. Nevertheless, for a clearer understanding and detailed comparison of the results obtained for EP/PhBR and PhEP/PhBR composites, the results obtained for PhBR are also presented in this article (since PhBR was used as a matrix for the preparation of EP/PhBR and PhEP/PhBR composites).

3.1. FTIR Spectroscopy

To investigate the modification of EP through the OxCh reaction, the FTIR spectra of EP and PhEP were compared (Figure 4).

Preprints (www.preprints.org) | NOT PEER-REVIEWED | Posted: 20 October 2023 doi:10.20944/preprints202310.1338.v1

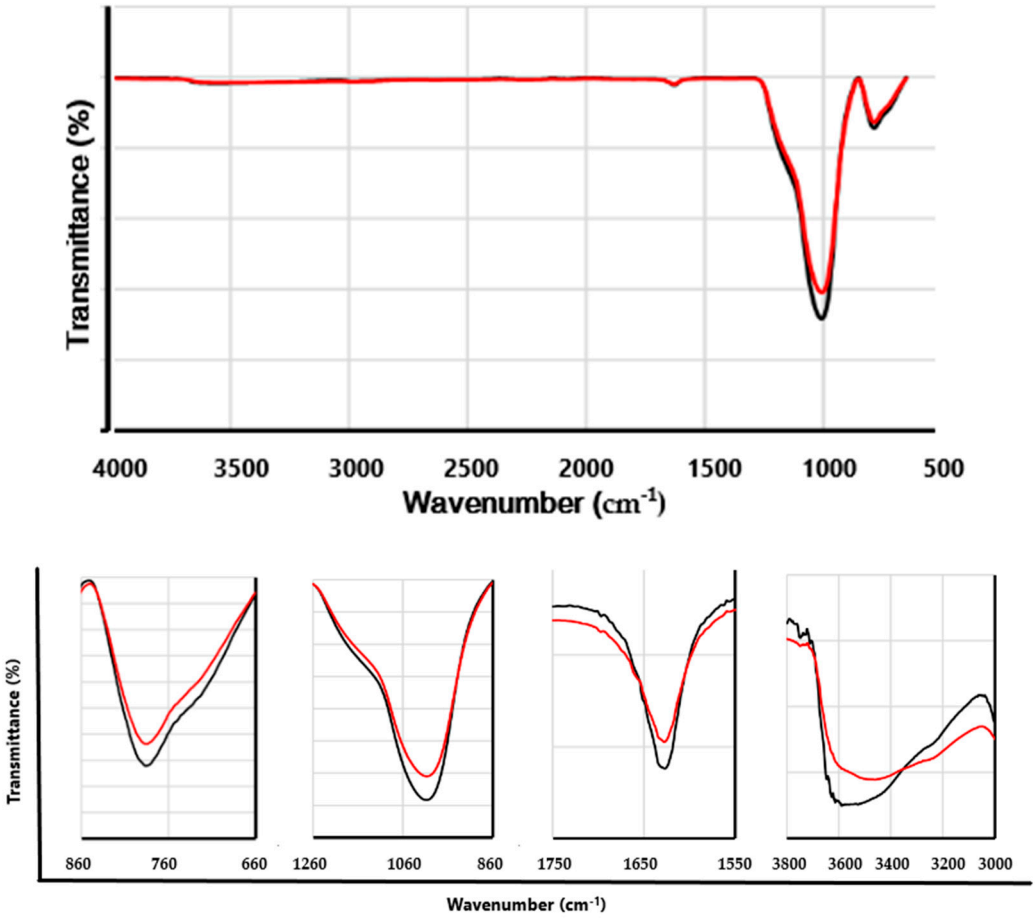

Figure 4. FTIR spectra of EP (black) and PhEP (red).

The FTIR spectrum of EP (black line) contains the following main absorption bands: 1628 cm^{-1}, 1000 cm^{-1}, and 787 cm^{-1}. In addition, a wide band is observed in the 3650-3350 cm-1 range. The strong band at 1000 cm^{-1} relates to the vibration of the Si-O bond, which is expected since the main constituent of the EP is silicon oxide (SiO_2). A broad band in the range of 3650-3350 cm^{-1} indicates axial deformation of the OH of Si-OH groups of the EP. The peak located at 787 cm^{-1} is attributed to the Si-O stretching vibration of Si-O-Al. The peak at 1628 cm^{-1} is attributed to adsorbed water [20,21].

In the FTIR spectrum of PhEP (red line), it was observed that the absorption band around 1000 and 787 cm^{-1}, associated with the bond vibration of the Si-O groups present in the unmodified EP, became more oval. In addition, small shoulders are visible in the range of 787-758 cm^{-1} and 1083-1000 cm^{-1}. There was probably an overlap of bands associated with modified silanol groups and absorption bands associated with P=O and P-OH groups, which are located almost in the region of 810-1100 cm^{-1} [16–18,22]. The spectrum also shows a relatively broad band in the range from 3100 to 3600 cm^{-1}, due to the OH stretching absorption of the -$P(O)(OH)_2$ groups [16]. All these observations confirm that the phosphoric acid groups have functionalized the EP surface, although not deeply.

In general, over the entire interval, the PhEP absorption bands had lower intensity than the EP. This result was obtained when EP was treated with alkali [23].

The spectra of PhBR and composites are presented in Figure 5.

Preprints (www.preprints.org) | NOT PEER-REVIEWED | Posted: 20 October 2023 doi:10.20944/preprints202310.1338.v1

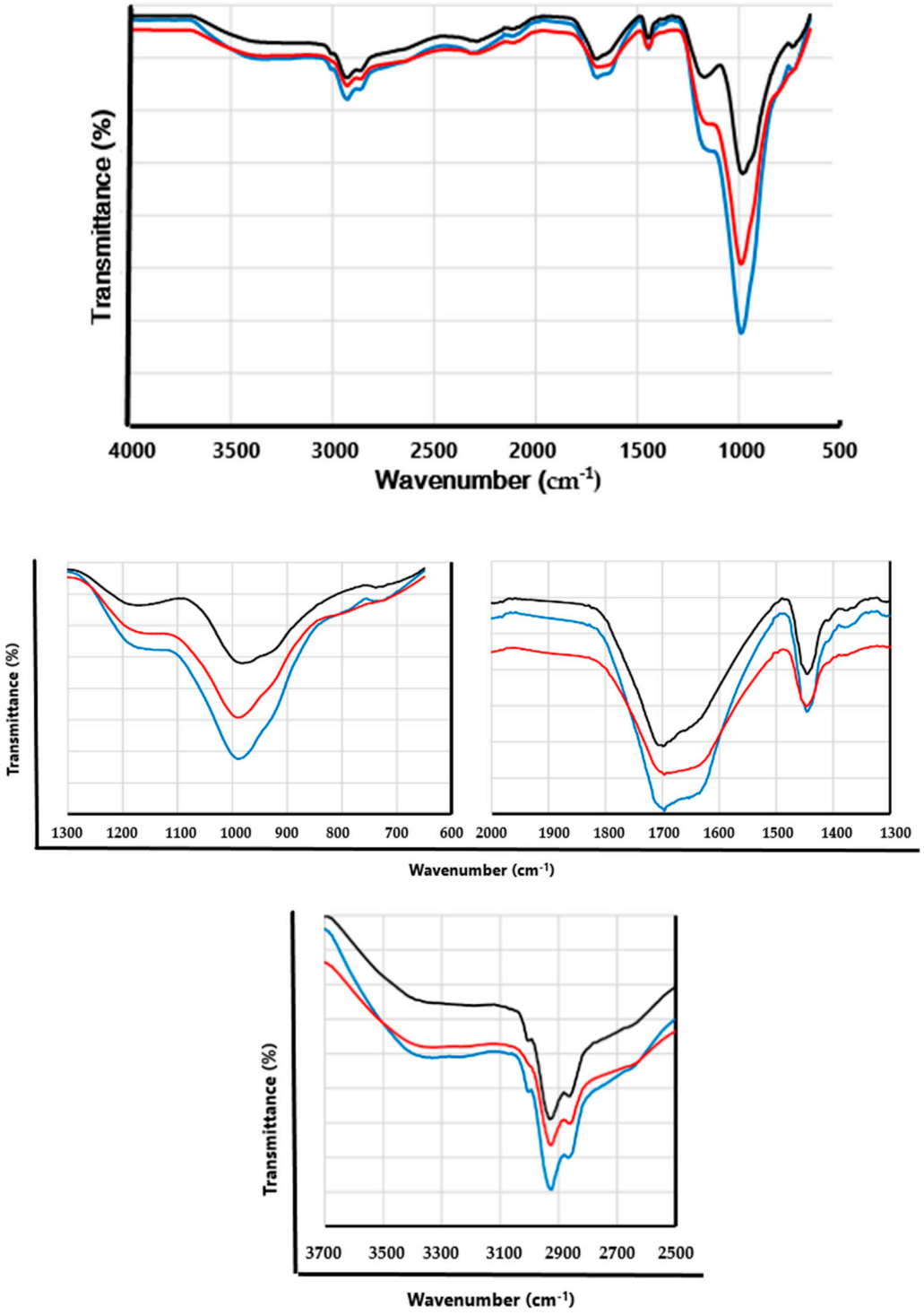

Figure 5. FTIR spectra of PhBR (black), EP/PhBR (blue), and PhEP/PhBR (red) composites.

As mentioned in our previous work, PhBR is characterized mainly by the following functional groups: P=O, –P(O)(OH)$_2$, P–OH. The band appearing at 1180 cm^{-1} can be attributed to vibrations of the P=O groups. The IR bands at 1702, 2864, and 3394 cm^{-1} are attributed to the -OH vibration in –PO(OH)$_2$ groups. An intensive band at 986 cm^{-1}, corresponding to the C–O–P bond, indicates the attachment of the –PO(OH)$_2$ groups to the macromolecular chain via oxygen. The absorption band of the P–OH group can also appear in the 900–950 cm^{-1}, which is observed in the form of a shoulder at 926 cm^{-1}. In addition, CH$_2$ groups include clearly visible bands in the range of 1400-1500 cm^{-1}, which is characteristic of BR [24].

 doi:10.20944/preprints202310.1338.v1

As can be seen from the figure, the spectra of the composites (Figure 5, blue and red lines) contain absorption bands characteristic of both PhBR and PhEP, but of course, with some changes. This confirms that the composites consist of BR and EP.

In the spectra of composites, it was observed that the absorption band at 1000 cm^{-1}, associated with the vibration of the Si-O bond of the group present in the unmodified EP is shifted lower wavenumber, in this case, the band appears at 994 cm^{-1}. This may be due to the formation of hydrogen bonds between the functional groups of the PhEP and the PhBR. This is also supported by the fact that the shoulder present in the PhBR spectrum (at 926 cm^{-1}) is practically invisible in composites. This means that the P–OH groups present in the PhBR are involved in the polymer-mineral interaction in the composites. The absorption band in the range of 980–1000 cm^{-1} in the composites is more intense than in PhBR. There was probably an overlap between the bands of silanol groups in PhEP and the absorption bands of the C–O–P bond, which are practically in the same spectral region.

In the range of 1050-1200 cm^{-1}, the spectra of the composites differ from the spectrum of PhBR, namely, the intensity of the absorption band present at 1180 cm^{-1} (related to P=O groups) is significantly reduced in the composites. This is explained by the fact that in composites a hydrogen bond is formed at the oxygen of the phosphoryl group.

In general, when comparing the spectra of the composites and PhBR, it is clear that the following pattern is observed in the intensity of absorption bands:

Intensity (PhBR) < Intensity (PhEP/PhBR) < Intensity (EP/PhBR)

Namely, over the entire range, the absorption band of the first type composite (EP/PhBR) is more intense than that of the second type composite (PhEP/PhBR). According to the synthesis conditions, EP in the PhEP/PhBR composite should be more modified. These results are in good agreement with the data presented in Figure 4. According to the FTIR spectra, the corresponding absorption bands in the PhEP have lower intensity.

3.2. UV-Vis Spectroscopy

By studying the optical properties of the samples, it is possible to make an opinion about their possible application areas in the future. For example, with UV-Vis studies, certain ideas can be given about the photocatalytic activity of materials, and for this purpose, UV-Vis studies were also conducted. The study of absorption spectra is a method of learning more information about the structure of a material.

Figure 6 shows the UV-Vis spectra of EP and PhEP (a), EP/PhBR and PhEP/PhBR composites (b) and PhBR (c). As can be seen from the figure, after the OxCh reaction of EP, the observed peak at 254 nm wavelength shifted to smaller wavelengths (243 nm), and visible-light absorption was improved. This change can be caused by quantum size effects [25]. A similar phenomenon was also observed in g-C_3N_4 grafted expanded perlite [26].

As can be seen from the UV-Vis spectra of EP/PhBR and PhEP/PhBR composites (Figure 6 (b)) and PhBR (Figure 6 (c)), all samples have strong absorption in the visible light region. It is interesting that, unlike PhBR, a red shift was observed in the UV-Vis spectrum of EP/PhBR, and a blue shift was observed in the UV-Vis spectrum of PhEP/PhBR. The red shift in the UV-Vis spectrum of EP/PhBR is related to the incorporation of EP into the PhBR matrix and has been observed in composite materials in many research studies [27,28]. This may also be due to the formation of an H-bond between –OH of EP and O=P– in phosphoric acid groups of PhBR. A similar situation was observed in the composites formed due to the H-bond between the amine groups of polyaniline and the hydroxyl groups of Fe_3O_4 [29]. It is known from the literature that when PVA is functionalized with phosphate groups, a blue shift is observed in the UV-Vis spectrum [30]. PhEP has phosphate groups, which indicates that the amount of phosphate groups in PhEP/PhBR is higher than that of PhBR and EP/PhBR. Thus, the blue shift observed in PhEP/PhBR may also be due to phosphate groups. This can also be seen from the SEM results (Figure 12).

Preprints (www.preprints.org) | NOT PEER-REVIEWED | Posted: 20 October 2023 doi:10.20944/preprints202310.1338.v1

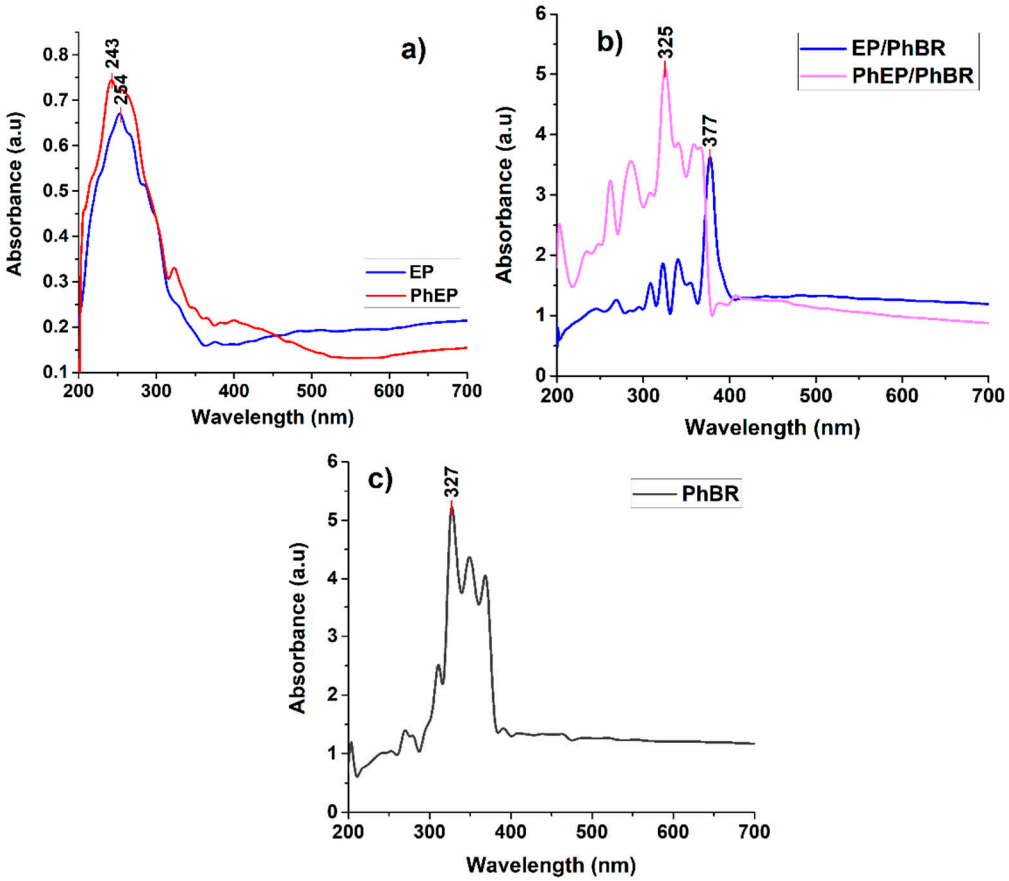

Figure 6. UV-visible spectra of EP and PhEP (a), EP/PhBR and PhEP/PhBR composites (b) and PhBR (c).

The optical band gap of the samples was calculated based on the Tauc formula [31]:

$$(\alpha h\nu)^n = C(h\nu - E_g)$$

where h is Planck's constant, C is constant, ν is the frequency, E_g is the optical band gap, α absorption coefficient, n is 1/2 in the case of direct allowed transitions, and 2 for indirect allowed transitions.

It can be seen from Figure 7 that the optical band gap of PhEP (3.43 eV) is smaller than the optical band gap of EP (3.59 eV). That is, the effect of the acids obtained during the OxCh reaction and the hydrolysis of the intermediate product on the EP led to a decrease in its optical band gap. Reduction of the optical band gap was also observed in acid-activated bentonite under microwave irradiation with hydrochloric and sulfuric acids to obtain photocatalytic activity [32].

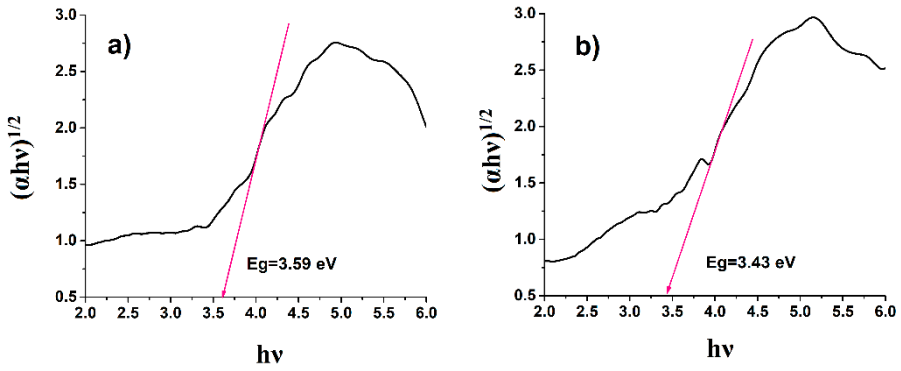

Figure 7. Optical band gap calculation of EP (a) and PhEP (b).

Preprints (www.preprints.org) | NOT PEER-REVIEWED | Posted: 20 October 2023 doi:10.20944/preprints202310.1338.v1

Different situations were observed in the two composites obtained based on PhBR. The addition of EP decreased the optical band gap to 3.00 eV in PhBR (Figure 8 (b)). However, the optical band gap was increased after the combination of PhEP and PhBR to 3.27 eV (Figure 8 (c)). This phenomenon can be explained as follows. It is known from the literature that the width of the optical band of polyvinyl alcohol films modified with phosphoric acid increases as the concentration of the acid increases. Because there is a relationship between the concentration of phosphoric acid and the amount of defects in the films. The amount of defects in films decreases with excess concentration of phosphoric acid. It is known that defects in films form localized states in the optical band gap, and these localized states overlap. If the overlap in localized states decreases, the energy band gap increases due to the increase in phosphoric acid concentration in the polymer matrix [33]. Based on the above, the following conclusions can be drawn: In the PhEP/PhBR composite, EP was initially modified by the OxCh reaction. This indicates that there is a chemical affinity between the polymer and mineral components in this type of composite and that there are fewer structural defects in the composite. As a result, an increase in the optical band gap is observed; in the EP/PhBR composite, the inclusion of EP in the PhBR matrix led to the formation of structural defects and, as a result, reduced the optical band gap.

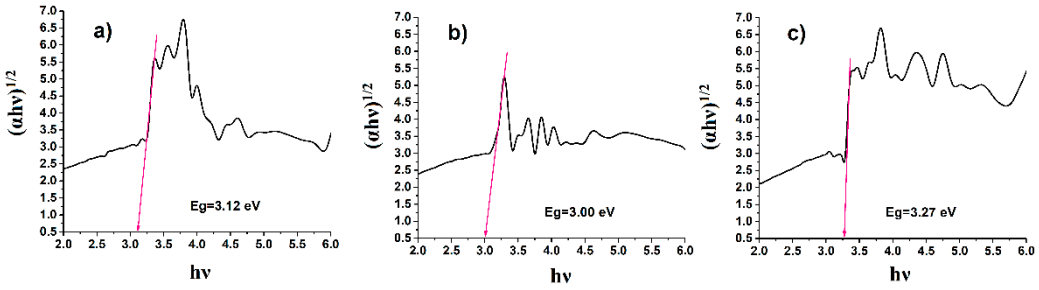

Figure 8. The optical band gap calculations of PhBR (a), EP/PhBR (b), and PhBR/PhBR (c) composites.

3.3. XRD Analysis

XRD analysis of the EP sample was usually performed to confirm the presence of ordered (e.g., zeolite) or disordered (e.g., amorphous silica) oxide materials [23]. XRD patterns of EP and PhEP samples are given in Figure 9. As can be seen from the figure, EP consists of an amorphous mineral phase (amorphous silica (SiO_2)), with glassy mass observed between 10° and 40° values of 2θ. After the OxCh reaction of EP, the diffraction peak corresponding to the amorphous phase was not changed in shape, and this indicates no change in the porous structure of the EP during modification and the phosphorus-containing groups attached to the surface of EP. However, after the OxCh reaction of EP, a new crystalline peak was observed at the value of 24.6° of 2θ [34]. The increase in the intensity of the peak at the value of 24.6° of 2θ after the OxCh reaction can be explained as follows: It is known from the literature that the composition of EP consists of SiO_2, Al_2O_3, CaO, MgO, Fe_2O_3, Na_2O, K_2O oxides and trace amounts of metal oxides [35]. HCl and H3PO4 acids released when hydrolyzing the modification obtained from the OxCh reaction of EP can react with amphoteric and basic oxides in expanded perlite and reduce the amount of these oxides because of washing. At this time, the amount of SiO_2 acid oxide, which does not react with acids, increases compared to other oxides in the material. Based on literature data, the peak observed at 2θ value of 24.6° can be attributed to amorphous SiO_2 [23]. A similar phenomenon was observed in the XRD patterns of the product obtained from the modification of EP with NaOH and HCl [23]. The noted diffraction peak has also been observed by several authors [36,37] at values close to 2θ and is a good match with JCPDS data (card No. 01-086-1561) [38].

Preprints (www.preprints.org) | NOT PEER-REVIEWED | Posted: 20 October 2023 doi:10.20944/preprints202310.1338.v1

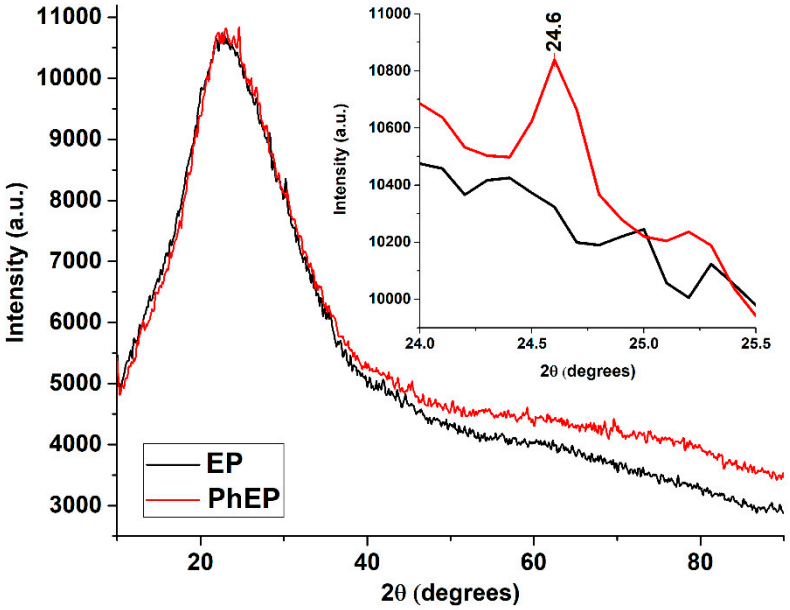

Figure 9. XRD spectra of EP and PhEP.

XRD patterns of PhBR, EP/PhBR, and PhEP/PhBR composite samples are given in Figure 10. As can be seen from the figure, in the XRD patterns of PhBR, EP/PhBR, and PhEP/PhBR composite samples, diffraction peaks corresponding to the amorphous phase are observed between 10° and 40° angles of 2θ. Additionally, these peaks corresponding to the amorphous phase are similar for the PhBR, EP/PhBR, and PhEP/PhBR composite samples, and no new diffraction peaks were observed. This indicates that the porous structure of EP is not changed in both EP/PhBR and PhEP/PhBR composites.

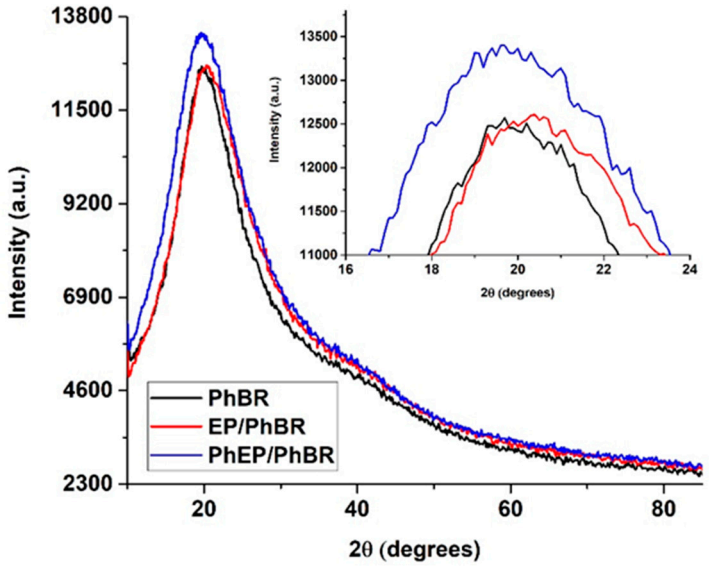

Figure 10. XRD spectra of PhBR, EP/PhBR, and PhEP/PhBR composites.

Comparing the XRD patterns of PhBR and EP/PhBR composite samples (Figure 10), it can be seen that the observed amorphous halo is broader in EP/PhBR composite than in PhBR and shifted to higher angles of 2θ. This may be due to the formation of a new amorphous phase in the PhBR matrix by the addition of EP. A similar situation was observed in perlite and geopolymer synthesized from perlite [34].

Preprints (www.preprints.org) | NOT PEER-REVIEWED | Posted: 20 October 2023 doi:10.20944/preprints202310.1338.v1

As can be seen from the comparison of XRD patterns of EP/PhBR and PhEP/PhBR composites (Figure 10), the amorphous halo observed between 10° and 40° values of 2θ is more intense in PhEP/PhBR composite than in EP/PhBR composite. This may be related to the chemical bonding formations between the filler and the polymer matrix in the PhEP/PhBR composite. Because PhEP has better dispersion and interaction with the PhBR matrix than EP, and this may be due to the presence of phosphorus-containing acidic groups on the surface of PhEP. A similar situation was obtained in the results of XRD studies of EP/acrylonitrile-butadiene-styrene composite [2].

3.4. SEM-EDX Analysis

Figures 11 and 12 illustrate the results of SEM-EDX analysis of samples.

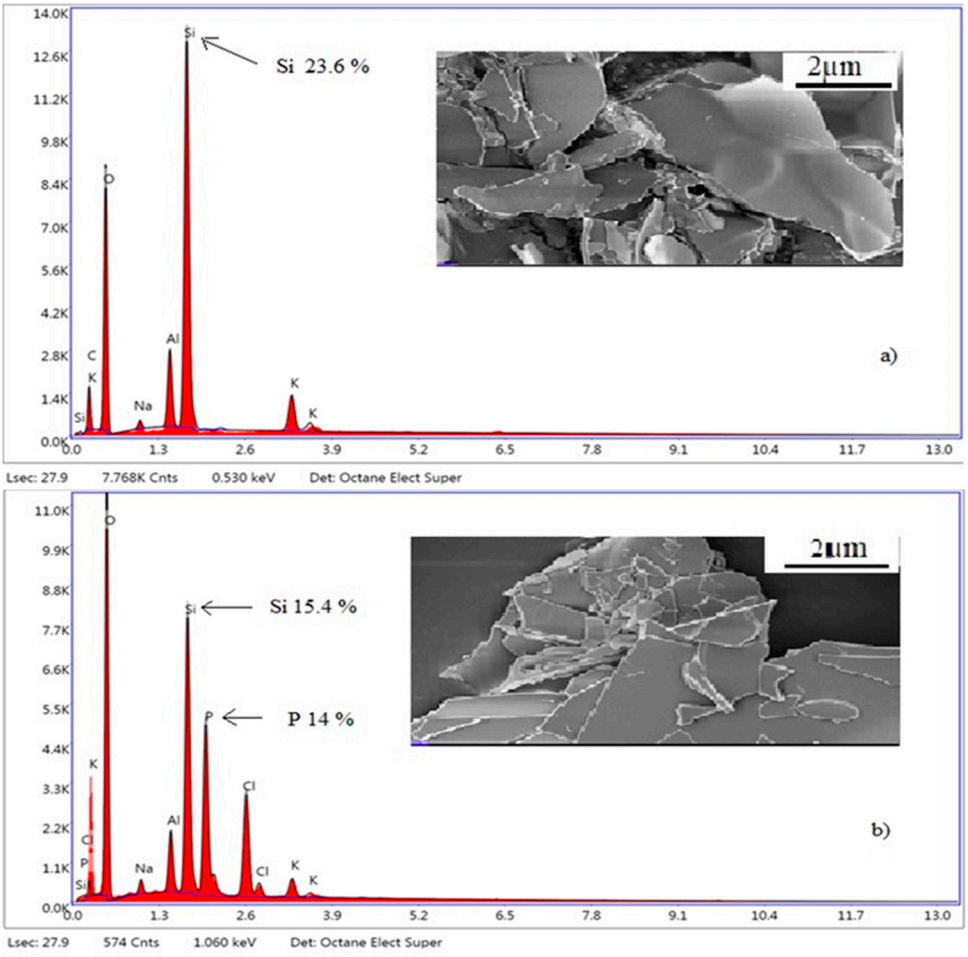

Figure 11. SEM-EDX micrographs of EP (a) and PhEP (b).

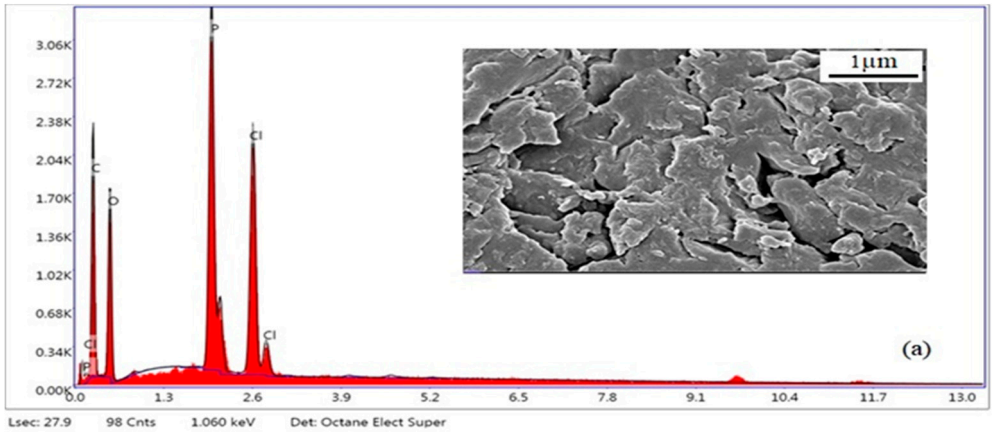

Preprints (www.preprints.org) | NOT PEER-REVIEWED | Posted: 20 October 2023 doi:10.20944/preprints202310.1338.v1

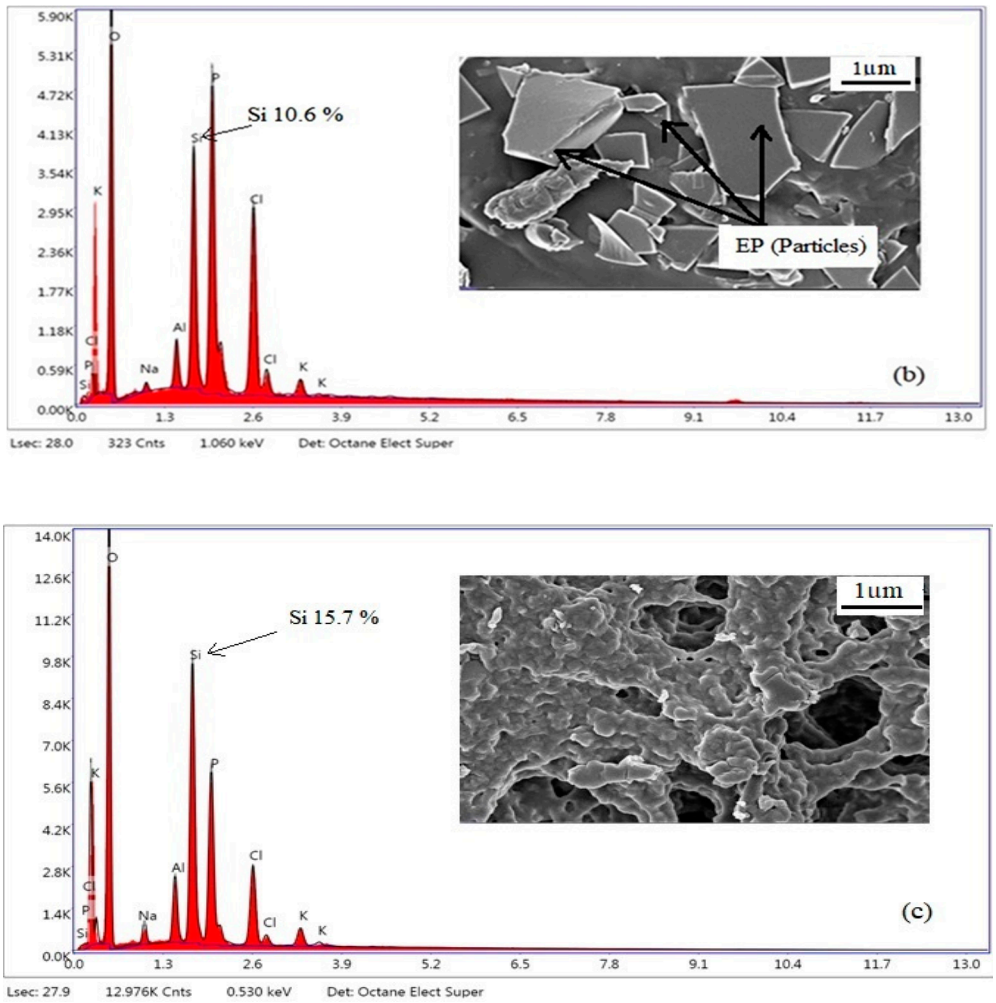

Figure 12. SEM-EDX micrographs of PhBR (a), EP/PhBR composite (b), and PhEP/PhBR composite (c).

As can be seen from Figure 11, compared to the EP, PhEP has a clearly defined layered structure. Apparently, during the OxCh reaction, impurities (mainly oxides of sodium, potassium, etc. and they are visible in the SEM analysis as small particles) were modified, and soluble salts were removed from the EP by water treatment. According to the results of EDX analysis, the PhEP contains phosphorus and chlorine atoms, i.e., during the reaction, EP unambiguously undergoes modification.

When considering the results of the SEM-EDX analysis presented in Figure 12, it is clearer that, unlike PhBR, composites contain both a polymer and a mineral phase. When comparing the morphology of composites of the first (EP/PhBR) and second (PhEP/PhBR) types, the difference can be clearly emphasized. Apparently, in the first type of composite, the EP undergoes a relatively low degree of modification, therefore, in the morphology of this sample, EP layers are clearly visible (which is in good agreement with the results of FTIR analysis), and the polymer is distributed around it. Figure 12 (c) demonstrated an indistinct difference between the PhEP particles and the polymer matrix, indicating good dispersion of the PhEP filler into the matrix, resulting in a homogeneous PhEP/PhBR composite. This difference is related to the synthesis conditions.

In the synthesis of the first type of composite (EP/PhBR), EP and BR are added to the reaction flask simultaneously and the OxCh reaction is carried out. Thus, it was determined that insufficient dispersion was achieved in the composite synthesized by this approach. During the preparation of the second type of composition (PhEP/PhBR), EP is first added to the reaction flask, its initial modification is carried out, then the polymer solution is added to the reaction mixture and the OxCh reaction is carried out. Therefore, premodification of EP provides a better dispersion of the mineral in the composite.

5. Conclusions

Polymer/mineral composites containing BR and EP were prepared by OxCh and hydrolysis of the intermediate product was obtained after this reaction. In this research work, EP, its phosphorus-containing derivative (PhEP), phosphorus-containing BR (PhBR), and two types of composites based on EP, PhEP, and PhBR, namely EP/PhBR and PhEP/PhBR, were characterized by various methods. To design the first type of EP/PhBR composite, EP and BR were simultaneously modified, and to design the second type of PhEP/PhBR composite, initially, the EP was modified by the OxCh reaction, and then the modification was continued in the presence of BR. The results of FTIR spectroscopy showed the presence of P=O, P-OH, and -P(O)$(OH)_2$ groups in PhBR, PhEP, and both composites. The results of the UV-Vis study were used to calculate the optical band gap for the samples. Based on the obtained results, the value of the E_g parameter was determined as follows: EP/PhBR<PhBR<PhEP/PhBR. These results indicate a greater chemical affinity between the polymer and mineral phases in the PhEP/BR composite. XRD studies have shown that both the modification of EP and the removal of contaminants by the OxCh reaction are effective. Comparison of XRD results of PhBR, EP/PhBR, and PhEP/PhBR composite showed better dispersion and interaction of mineral phase in the polymer matrix in PhEP/PhBR. The results of SEM-EDX analysis show that the PhEP has a more distinct layered structure. Apparently, impurities were removed from the EP during the OxCh reaction. According to the results of EDX analysis, phosphorus, and chlorine atoms are also present in PhEP. Based on the results of SEM-EDX analysis, it was established that, unlike PhBR, composites contain both a polymer and a mineral phase. In addition, preliminary modification of EP makes it possible to obtain a composite (the second type of PhEP/PhBR composite) with good mineral dispersion.

Author Contributions: N.E. and R.A. wrote the manuscript; I.B.-z., M.S., S.T., N.B., N.G and S.M. conducted the experiment; S.A. participated in the interpretation of the experimental results, writing and editing the article. All authors have read and agreed to the published version of the manuscript.

Funding: This research received no external funding.

Acknowledgments: Nada Edres is extremely grateful to the Azerbaijan scholarship for citizens of Organisation of Islamic Cooperation member countries for financial support and for giving the chance to join the research group of Prof Rasim Alosmanov in the Department of Chemistry of High molecular compounds, Faculty of Chemistry, Baku State University.

Conflicts of Interest: The authors have no conflict of interest to declare that are relevant to the content of this article

References

1. Samar, M.; Saxena, D.S. Study of Chemical of and Chysical Properties of Perlite and Its Application in India. *Int. J. Sci. Technol. Manag.* **2016**, *5*, 70–80.
2. Gül, D. Characterization and Expansion Behaviour of Perlite. Master Thesis, Izmir Institute of Technology, 2016.
3. Aksoy, O.; Alyamac Seydibeyoglu, E.; Mocan, M.; Sutcu, M.; Ozveren-Ucar, N.; Seydibeyoglu, M. Characterization of Perlite Powders from Izmir, Türkiye Region. *Physicochem. Probl. Miner. Process.* **2022**, doi:10.37190/ppmp/155277.
4. Różycka, A.; Pichór, W. Effect of Perlite Waste Addition on the Properties of Autoclaved Aerated Concrete. *Constr. Build. Mater.* **2016**, *120*, 65–71, doi:10.1016/j.conbuildmat.2016.05.019.
5. Kotwica, Ł.; Pichór, W.; Kapeluszna, E.; Różycka, A. Utilization of Waste Expanded Perlite as New Effective Supplementary Cementitious Material. *J. Clean. Prod.* **2017**, *140*, 1344–1352, doi:10.1016/j.jclepro.2016.10.018.
6. Wang, L.; Li, Z.; Jing, Q.; Liu, P. Synthesis of Composite Insulation Materials—Expanded Perlite Filled with Silica Aerogel. *J. Porous Mater.* **2018**, *25*, 373–382, doi:10.1007/s10934-017-0448-4.
7. Xu, H.; Jia, W.; Ren, S.; Wang, J. Novel and Recyclable Demulsifier of Expanded Perlite Grafted by Magnetic Nanoparticles for Oil Separation from Emulsified Oil Wastewaters. *Chem. Eng. J.* **2018**, *337*, 10–18, doi:10.1016/j.cej.2017.12.084.
8. Guo, F.; Aryana, S.; Han, Y.; Jiao, Y. A Review of the Synthesis and Applications of Polymer–Nanoclay Composites. *Appl. Sci.* **2018**, *8*, 1696, doi:10.3390/app8091696.

9. Raji, M.; Nekhlaoui, S.; El Hassani, I.-E.E.A.; Essassi, E.M.; Essabir, H.; Rodrigue, D.; Bouhfid, R.; Qaiss, A.E.K. Utilization of Volcanic Amorphous Aluminosilicate Rocks (Perlite) as Alternative Materials in Lightweight Composites. *Compos. Part B Eng.* **2019**, *165*, 47–54, doi:10.1016/j.compositesb.2018.11.098.
10. Krzyzak, A.; Kucharczyk, W.; Gaska, J.; Szczepaniak, R. Ablative Test of Composites with Epoxy Resin and Expanded Perlite. *Compos. Struct.* **2018**, *202*, 978–987, doi:10.1016/j.compstruct.2018.05.018.
11. Abir, A.; Faruk, M.; Arifuzzaman, M. *Novel Expanded Perlite Based Composite Using Recycled Expanded Polystyrene for Building Material Applications*; 2020;
12. Atagür, M.; Sarikanat, M.; Uysalman, T.; Polat, O.; Elbeyli, İ.Y.; Seki, Y.; Sever, K. Mechanical, Thermal, and Viscoelastic Investigations on Expanded Perlite–Filled High-Density Polyethylene Composite. *J. Elastomers Plast.* **2018**, *50*, 747–761, doi:10.1177/0095244318765045.
13. Ghorbankhan, A.; Nakhaei, M.R.; Safarpour, P. Fracture Behavior, Microstructure, and Mechanical Properties of PA6 / NBR Nanocomposites. *Polym. Compos.* **2022**, *43*, 6696–6708, doi:10.1002/pc.26993.
14. Akkaya, R.; Akkaya, B. New Low-Cost Composite Adsorbent Synthesis and Characterization. *Desalination Water Treat.* **2013**, *51*, 3497–3504, doi:10.1080/19443994.2012.749374.
15. Akkaya, R. Synthesis and Characterization of a New Low-Cost Composite for the Adsorption of Rare Earth Ions from Aqueous Solutions. *Chem. Eng. J.* **2012**, *200–202*, 186–191, doi:10.1016/j.cej.2012.06.042.
16. Alosmanov, R.; Wolski, K.; Matuschek, G.; Magerramov, A.; Azizov, A.; Zimmermann, R.; Aliyev, E.; Zapotoczny, S. Effect of Functional Groups on the Thermal Degradation of Phosphorus- and Phosphorus/Nitrogen-Containing Functional Polymers. *J. Therm. Anal. Calorim.* **2017**, *130*, 799–812, doi:10.1007/s10973-017-6464-4.
17. Aliyeva, S.; Alosmanov, R.; Buniyatzadeh, I.; Eyvazova, G.; Azizov, A.; Maharramov, A. Functionalized Graphene Nanoplatelets/Modified Polybutadiene Hybrid Composite. *Colloid Polym. Sci.* **2019**, *297*, 1529–1540, doi:10.1007/s00396-019-04565-8.
18. Aliyeva, S.; Maharramov, A.; Azizov, A.; Alosmanov, R.; Buniyatzadeh, I.; Eyvazova, G. Phosphorus-Containing Polybutadiene Rubber–Bentonite Hybrid Composite for the Removal of Rhodamine 6G from Water. *Anal. Lett.* **2016**, *49*, 2347–2364, doi:10.1080/00032719.2016.1139586.
19. Alosmanov, R.M.; Azizov, A.A.; Magerramov, A.M. NMR Spectroscopic Study of Phosphorus-Containing Polymer Sorbent. *Russ. J. Gen. Chem.* **2011**, *81*, 1477–1479, doi:10.1134/S1070363211070127.
20. Jahanshahi, R.; Akhlaghinia, B. Expanded Perlite: An Inexpensive Natural Efficient Heterogeneous Catalyst for the Green and Highly Accelerated Solvent-Free Synthesis of 5-Substituted-1H-Tetrazoles Using [Bmim]N 3 and Nitriles. *RSC Adv.* **2015**, *5*, 104087–104094, doi:10.1039/C5RA21481E.
21. Almeida, J.M.F.; Silva, I.N.; Damasceno Junior, E.; Fernandes, N.S. Modification of Expanded Perlite with Orthophenanthroline for Formation of Active Sites for Acid Dyes: Preparation and Characterization. *Periód. Tchê Quím.* **2018**, *15*, 338–346, doi:10.52571/PTQ.v15.n30.2018.341_Periodico30_pgs_338_346.pdf.
22. Alosmanov, R.; Buniyat-zadeh, I.; Soylak, M.; Shukurov, A.; Aliyeva, S.; Turp, S.; Guliyeva, G. Design, Structural Characteristic and Antibacterial Performance of Silver-Containing Cotton Fiber Nanocomposite. *Bioengineering* **2022**, *9*, 770, doi:10.3390/bioengineering9120770.
23. Wheelwright, W.; Cooney, R.P.; Ray, S.; Zujovic, Z.; De Silva, K. Ultra-High Surface Area Nano-Porous Silica from Expanded Perlite: Formation and Characterization. *Ceram. Int.* **2017**, *43*, 11495–11504, doi:10.1016/j.ceramint.2017.05.333.
24. Alghadi, A.M.; Tirkes, S.; Tayfun, U. Mechanical, Thermo-Mechanical and Morphological Characterization of ABS Based Composites Loaded with Perlite Mineral. *Mater. Res. Express* **2020**, *7*, 015301, doi:10.1088/2053-1591/ab551b.
25. Aubert, T.; Golovatenko, A.A.; Samoli, M.; Lermusiaux, L.; Zinn, T.; Abécassis, B.; Rodina, A.V.; Hens, Z. General Expression for the Size-Dependent Optical Properties of Quantum Dots. *Nano Lett.* **2022**, *22*, 1778–1785, doi:10.1021/acs.nanolett.2c00056.
26. Zhang, S.; Li, H.; Yang, Z. Synthesis, Structural Characterization and Evaluation of a Novel Floating Metal-Free Photocatalyst Based on g-C 3 N 4 Grafted Expanded Perlite for the Degradation of Dyes. *Mater. Technol.* **2018**, *33*, 1–9, doi:10.1080/10667857.2017.1367148.
27. Abbas, M.; Hachemaoui, A.; Yahiaoui, A.; Mourad, A.-H.I.; Belfedal, A.; Cherupurakal, N. Chemical Synthesis of Nanocomposites via In-Situ Polymerization of Aniline and Iodoaniline Using Exchanged Montmorillonite. *Polym. Polym. Compos.* **2021**, *29*, 982–991, doi:10.1177/0967391120954069.
28. Lee, J.Y.; Cui, C.Q. Electrochemical Copolymerization of Aniline and Metanilic Acid. *J. Electroanal. Chem.* **1996**, *403*, 109–116, doi:10.1016/0022-0728(95)04215-6.
29. Hsieh, T.-H.; Ho, L.-C.; Wang, Y.-Z.; Ho, K.-S.; Tsai, C.-H.; Hung, L.-F. New Inverse Emulsion-Polymerized Iron/Polyaniline Composites for Permanent, Highly Magnetic Iron Compounds via Calcination. *Polymers* **2021**, *13*, 3240, doi:10.3390/polym13193240.
30. Mohamed Saat, A.; Alaauldin, S.; Kamil, M.S.; Zainal Azaim, F.Z.; Johan, M.R. The Optical Properties of Polyvinyl Alcohol (PVA), Phosphorylated Polyvinyl Alcohol (PPVA), and Phosphorylated Polyvinyl Alcohol—Aluminum Phosphate (PPVA-AlPO4) Nanocomposites: Effect of Phosphate Groups. In *Design in*

Maritime Engineering; Ismail, A., Dahalan, W.M., Öchsner, A., Eds.; Advanced Structured Materials; Springer International Publishing: Cham, 2022; Vol. 167, pp. 179–187 ISBN 978-3-030-89987-5.

31. Tauc, J.; Grigorovici, R.; Vancu, A. Optical Properties and Electronic Structure of Amorphous Germanium. *Phys. Status Solidi B* **1966**, *15*, 627–637, doi:10.1002/pssb.19660150224.
32. Surendra, B.S.; Nagaswarupa, H.P.; Anantharaju, K.S.; Anil Kumar, M.R.; Nagabhushana, H.; Shetty, K. Acid Activation of Bentonite Clay under Microwave Irradiation: Characterization, Cyclic Voltammetry and Photocatalytic Activity. *Mater. Today Proc.* **2018**, *5*, 22643–22651, doi:10.1016/j.matpr.2018.06.639.
33. Mohamed Saat, A.; Johan, M.R. Effect of Phosphoric Acid Concentration on the Optical Properties of Partially Phosphorylated PVA Complexes. *Int. J. Polym. Sci.* **2014**, *2014*, 1–8, doi:10.1155/2014/495875.
34. Saufi, H.; El Alouani, M.; Alehyen, S.; El Achouri, M.; Aride, J.; Taibi, M. Photocatalytic Degradation of Methylene Blue from Aqueous Medium onto Perlite-Based Geopolymer. *Int. J. Chem. Eng.* **2020**, *2020*, 1–7, doi:10.1155/2020/9498349.
35. Papadopoulos, A.P.; Bar-Tal, A.; Silber, A.; Saha, U.K.; Raviv, M. Inorganic and Synthetic Organic Components of Soilless Culture and Potting Mixes. In *Soilless Culture*; Elsevier, 2008; pp. 505–543 ISBN 978-0-444-52975-6.
36. Buga, M.-R.; Spinu-Zaulet, A.A.; Ungureanu, C.G.; Mitran, R.-A.; Vasile, E.; Florea, M.; Neatu, F. Carbon-Coated SiO2 Composites as Promising Anode Material for Li-Ion Batteries. *Molecules* **2021**, *26*, 4531, doi:10.3390/molecules26154531.
37. Sun, J.; Xu, Z.; Li, W.; Shen, X. Effect of Nano-SiO2 on the Early Hydration of Alite-Sulphoaluminate Cement. *Nanomaterials* **2017**, *7*, 102, doi:10.3390/nano7050102.
38. Matmin, J.; Affendi, I.; Endud, S. Direct-Continuous Preparation of Nanostructured Titania-Silica Using Surfactant-Free Non-Scaffold Rice Starch Template. *Nanomaterials* **2018**, *8*, 514, doi:10.3390/nano8070514.